

Precipitation hardening in Al-Cu-Mg alloys revisited

S.C. Wang*, M.J. Starink and N. Gao

Materials Research Group, School of Engineering Science, University of Southampton, SO17
1BJ, UK

* Corresponding author. Tel.: +44 23 8059 4638; E-mail address: wangs@soton.ac.uk

Abstract

Transmission electron microscopy, differential scanning calorimetry and hardness test have been used to study the precipitation sequence on artificial ageing of a stretched Al-Cu-Mg alloy. Two ageing temperatures at 190°C and 150°C for different times have been chosen. Some orthorhombic GPB2/S" is present in samples aged at 150°C for 48h, which is at the very start of the 2nd stage of hardening. The combined experiments clearly show the second stage hardening is dominated by S phase, which forms a dense precipitation at the peak hardness stage, whilst no significant amounts of other phases or zones are detected.

Keywords: Al-Cu-Mg alloy; precipitate; TEM; DSC; Hardness, Strengthening.

1. Introduction

The phenomenon of precipitation hardening was first discovered in an Al-4wt%Cu-0.6wt%Mg alloy by the German chemist Alfred Wilm in 1906. One of the most widely used alloys in aeronautical industry is 2024 (Al-4.2wt%Cu-1.5wt%Mg-0.6wt%Mn), which was introduced in the 1930's. When ageing is performed at sufficiently low temperature (typically below about 200°C), two distinct stages of precipitation hardening in Al-Cu-Mg alloys are observed, separated by a plateau. The first stage is a very fast increase after quench and accounts for about 60% of maximum hardening. The second stage is the rise to peak hardness. The origin of the initial rapid hardening is still in dispute. Mechanisms cited for the rapid age hardening of Al-Cu-Mg alloys are formation of Guinier-Preston-Bagaryatsky (GPB) zones [1], Cu-Mg co-clusters [2,3], a dislocation-solute interaction [4,5]. In the early work, the second stage of hardening was generally attributed to the formation of the S' or S phase [1]. In the 1980's, Cuisiat et al. [6] suggested that a distinct precipitate termed S'' was responsible for the peak hardness. In the 1990's, using atom-probe field ion microscopy, Ringer et al. [2,7] proposed that the second-stage hardening (peak) is due to the formation of GPB zones, which start to form near the end of the hardness plateau. Obviously there are some controversies to the mechanism of the hardening, both in the initial and peak stages. This paper aims to clarify the mechanism for the later stages of plateau stage and the peak hardening (2nd stage) using transmission electron microscopy (TEM) and differential scanning calorimetry (DSC).

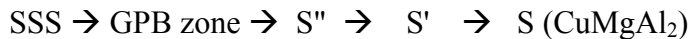
2. Experimental Procedure

An Al-2.81Cu-1.05Mg-0.41Mn (wt-%) alloy has been chosen. The Cu:Mg atomic ratio is close to 1. After solution treatment at 495°C, water quenching and stretching by 2.5%, the alloy has been left at room temperature for a few months (equivalent to T351 condition) before further ageing for 12-72 h at 150°C and for 6-48 h at 190°C respectively. Four indentations were made on each specimen with a 20 kg load and a mean HV is given. These corresponding treatments were also chosen for DSC and TEM investigation. DSC experiments were conducted at a constant heating rate of 10°C/min. All runs were corrected by subtracting the baseline of the DSC, which was obtained from a run with an empty pan as reference. Further baseline correction procedures are outlined in Ref. [8]. Disks of 3mm in diameter and around 0.25mm in thickness

were punched out from these slices, and subsequently electropolished using a solution of HNO₃ and methanol (1:3 in volume). TEM foils were examined using a JEOL 2000FX microscope operating at 200kV.

3. Ageing sequences

In order to understand the hardening mechanisms, it is necessary to briefly review the precipitation sequence during the ageing. Bagaryatsky [9] proposed the following precipitation sequence:



where SSS stands for supersaturated solid solution.

Different models for the S phase have been reported [10], but the most accepted structure for S phase is Perlitz and Westgren (P-W) model [11]. As S' has the same structure to S phase with slight difference in their lattice parameters, it is now regarded that there is no distinction between the S' and S phases.

The existence of a phase different from S or GPB (termed S'' or GPB2) has been disputed [10], and various crystallographic structures have been reported [6,9,10,12,13]. Charai et al. [12] and Kovarik et al. [13] reported HREM work indicating the presence of an intermediate phase termed S'' or GPB2. A new structure [14,15] was proposed for GPB2/S'' with the composition of Al₅(Cu,Mg)₃ and an orthorhombic structure (space group Imm2) and lattice parameters $a = 0.405$ nm, $b = 1.62$ nm and $c = 0.405$ nm, which elucidates both HREM images and the weak diffraction in TEM [15].

Evidence for the existence of the GPB zones was initially based on interpretations of weak diffraction effects arising from diffuse X-ray scattering [1,9]. However, a recent review has shown that evidence for the existence of the GPB zones is weak, and none of the models for Cu and Mg rich GPB zones presented since the 1950s [1,9,16,17] have been confirmed independently. Instead, recent work [2,4,18] using three-dimensional atom-probe (3DAP) shows that Cu-Mg co-clusters instead of GPB appear during initial ageing. During the first (rapid) stage of hardening no distinct precipitate can be detected by conventional TEM but DSC experiments clearly show a dissolution effect evidencing that a metastable pre-precipitate has formed [8,19].

Since there is no evidence for the existence of GPB, the following ageing sequence for S precipitates has been proposed [10]:

SSS → Cu-Mg clusters → GPB2/S" (orthorhombic) → S

4. Results and Analysis

Fig. 1 shows two curves of hardness vs ageing time for samples aged at 190°C and 150°C, respectively. It shows that ageing at 190°C for 6 hours is just short of peak ageing and 190°C for 12 hours is at peak ageing. Samples treated for 6 h and 12 h aged at 190°C have been chosen for TEM observation. Fig. 2 shows lath-shaped precipitates exist in both conditions. Simulated diffraction patterns, based on 12 variants of S phase [10] using the P-W model, match all spots in the $[112]_{Al}$ (Figs. 2b, 2c) and $[100]_{Al}$ SAD patterns (Figs. 2e, 2f). This indicates that S phase is the only precipitate after 6 hour ageing at 190°C. It is therefore concluded that S phase formation is the main reaction causing the rise in hardness in the second stage for the present Al-Cu-Mg which were stretched after quenching. Further evidence may be found from DSC results. As shown in Fig. 3, the dissolution peak has completely disappeared and the S phase formation effect has nearly disappeared after 6 h at 190°C. Further ageing causes little change in the DSC thermograms and hence we can conclude that after 6 h at 190°C the equilibrium phase (S) has formed.

Fig. 1 indicates that the sample is still in an under-aged state up to ageing for 72 hours at 150°C. Again, the corresponding samples studied in TEM. Before ageing for 12h at 150°C, there are no extra diffractions in SAD patterns (figure not presented), which means that Cu-Mg clusters detected by APFIM and DSC [3,8,10,18] dominate in this stage. After ageing for 24h at 150°C, the TEM bright field image (Fig. 4a) shows high contrast of defects in this stretched alloy but no precipitates can be resolved. However, the $[100]_{Al}$ SAD pattern (Fig. 4b) reveals faint reflections which are consistent with a combination of two phases: the orthorhombic GPB2/S" phase [14,15] and the S phase as illustrated in Fig. 4c. After ageing for 48h, a dense precipitation of S phase has occurred (Fig. 4d), and the intensity of diffractions from GPB2/S" seems to be reaching a maximum (Fig. 4e). Moreover, the existence of Ω precipitates has been identified (Fig. 4f). After ageing for 72h which is close to the second stage of hardening, GPB2/S" reflections are weaker and more S precipitates have formed (Figs. 4g-i). The above TEM results are consistent with DSC thermograms: Fig. 5a shows that the peaks for formation of S phase decreases with ageing time, which means samples aged for longer times contained more S phase precipitates. The dissolution effect of clusters+GPB2/S" reaches a maximum around 48 h and decrease again in 72

h, which is consistent with the maximum in intensity of SAD spots for GPB2/S" being reached in the sample aged for 48 h.

5. Discussion

There are some disputes on which precipitates contribute to the second hardening stage. In quenched and non-stretched alloys, the second stage of hardening has been interpreted to be due to GPB zones [2]. However, for the quenched and stretched Al-Cu-Mg alloy studied in the present work, DSC combined with TEM methods have shown that the second hardening peak corresponds to the completion of S phase formation, and S phase is the only ageing phase detected at this stage. This indicates that S phase formation is responsible for the second stage of hardening for quenched and stretched Al-Cu-Mg alloys. It could be argued that the difference between the observations by Ringer et al [2] and the present study is due to the stretch providing additional nucleation sites for S phase. However, other experiments on non-stretched Al-Cu-Mg alloys indicate also in non-stretched alloys significant S phase formation occurs during the second hardening stage. For example, Shih et al.'s experiments on a non-stretched Al-2.62Cu-1.35Mg (wt.-%) alloy [20] showed that ageing at 190°C for ~12 h was short of peak ageing (based on the hardness curve of Fig. 3 in [20]) the DSC indicated about ~85% of S phase formation was completed at this stage (based on the DSC curve of Fig. 5 in [20]), and 190°C for ~20 h was at peak ageing (based on the hardness curve of Fig. 3 in [20]) with fully completed formation of S phase (based on the DSC curve of Fig. 5 in [20]). This suggests the peak strengthening was related to the formation of S in Al-Cu-Mg alloys regardless of being stretched or not stretched. Nevertheless, the deformation increases the strength and shifts the peak for the S formation to lower temperature [21]. It is further noted that in alloys with a low dislocation density, lath and rod shaped S phase precipitates can form both on dislocations and in the matrix away from dislocations in the same sample. This has been evidenced for Al-Cu-Mg and Al-Cu-Mg-Li alloys [22,23].

We would here like to highlight that the previous inference of the presence of GPB zones could be unreliable: HREM images of precipitates, showing no clear crystal planes, were attributed previously to GPB zones [2]. In fact, the distorted HREM image of small S precipitates observed in $[100]_{\text{Al}}$ directions could be due to a deviation between the lattices of Al and S phase (5.4° or 3.3° [7]). This argument is further supported by an $[100]_{\text{Al}}$ SAD pattern (insert of Fig. 7a

of Ringer et al. [2]), which has the similar pattern as Fig. 2e indicating reflections mainly from S phase and Al matrix.

After ageing for 48 hours at 150°C, the intensity of diffraction spots (Fig 4e) indicate that the volume fraction of GPB2/S" is close to maximum, but the hardness is hardly changed (Fig. 1). Thus the strengthening contribution due to GPB2/S" formation is quite low in the present alloy. In other words, even though the orthorhombic GPB2/S" phase is detected in a limited window of ageing treatments, strengthening is always dominated by co-clusters and S phase.

In the sample aged at 150°C for 48 hours, SAD indicates the presence of Ω (Al₂Cu) phase (Fig 4e,f). The Ω phase has been commonly accepted as an orthorhombic [24] structure with lattice parameters of $a = 0.496$ nm, $b = 0.859$ nm, $c = 0.848$ nm. Ω phase formation has been reported to be stimulated by Ag and Si additions [10] and can form 2024 type alloys during a slow quench [25,26].

6. Conclusions

Previous evidence for GPB zones existing at the stage of peak hardness in Al-Cu-Mg alloys is very weak. Combination of hardness, TEM and DSC shows that in an Al-Cu-Mg alloy that is quenched, stretched and aged to peak strength, a dense precipitation of S phase occurs. At this stage, the S phase is the main contributor to the peak hardness. The orthorhombic S" or GPB2 is present in the latter stages of the plateau stage.

References

- [1] Silcock JM. J Inst Metals 1960-61;89:203.
- [2] Ringer SP, Sakurai T, Polmear IJ. Acta Mater 1997;45:3731.
- [3] Starink MJ, Gao N, Yan JL. Mater Sci Eng A 2004;387-389:222
- [4] Reich L, Ringer SP, Hono K. Phil. Mag. Lett 1999;79:639.
- [5] Nagai Y, Murayama M, Tang Z, Nonaka T, Hono K, Hasegawa M. Acta Mater 2001;49:913
- [6] Cuisiat F, Duval P, Graf R. Scripta Met 1984;18:1051.
- [7] Ringer SP, Hono K. Mater Characterization 2000;44:101
- [8] Starink MJ. Int Mater Rev 2004;49:191
- [9] Bagaryatshy YA. Dokl Akad SSSR 1952;87:397 & 559.
- [10] Wang SC, Starink MJ. Int Mater Rev 2005;50:193.

- [11] Perlitz H, Westgren A. Arkiv Kemi Mineral Geol 1943;16B:No13.
- [12] Charai A, Walther T, Alfonso C, Zahra AM, Zahra CY. Acta Mater 2000;48:2751.
- [13] Kovarik L, Gouma PI, Kisielowski C, Court SA, Mills MJ. Acta Mater 2004;52:2509.
- [14] Wang SC, Starink MJ. Inst of Phys Conf Ser 2004;179:277
- [15] Wang SC, Starink MJ. Mater Sci & Eng A 2004;386:156.
- [16] Wolverton C. Acta Mater 2001;49:3129.
- [17] Gerold V, H Haberkorn. Z Metall 1959;50:568.
- [18] Starink MJ, Gao N, Davin L, Yan J, Cerezo A. Phil Mag 2005;85:1395
- [19] Gao N, Davin L, Wang SC, Cerezo A, Starink MJ. Mater Sci Forum 2002;396-402:923.
- [20] Shih H, Ho N, Huang JC. Metall & Mater. Trans A 1996;27:2479.
- [21] Sen N, West, DRF. J Inst Met 1969;97:87
- [22] Starink MJ, Wang P, Sinclair I, Gregson PJ. Acta Mater. 1999; 47:3841
- [23] Starink MJ, Gregson PJ. Mater. Sci. Eng. A; 1996; 211:54
- [24] Knowles KM, Stobbs WM. Acta Cryst 1988;44B:207.
- [25] Wang LM, Flower HM, Lindley TC. Scripta Mater 1999;41:391.
- [26] Lefebvre F, Wang S, Starink MJ, Sinclair I. Mater Sci For 2002;396-4:1555

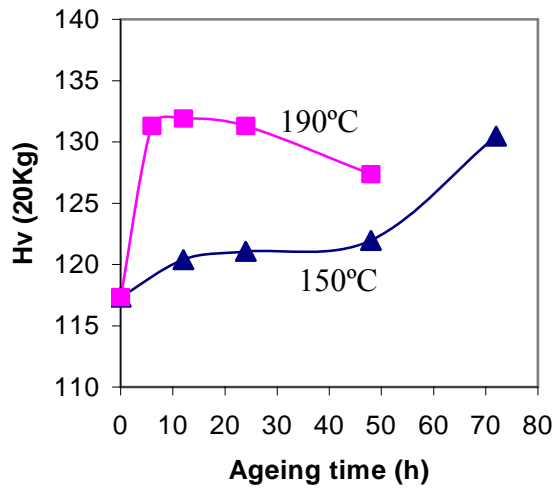


Fig.1 Hardness vs. ageing time curves of the quenched and stretched (T351) Al-2.81Cu-1.05Mg-0.41Mn (wt-%) alloy ageing at 190°C and 150°C.

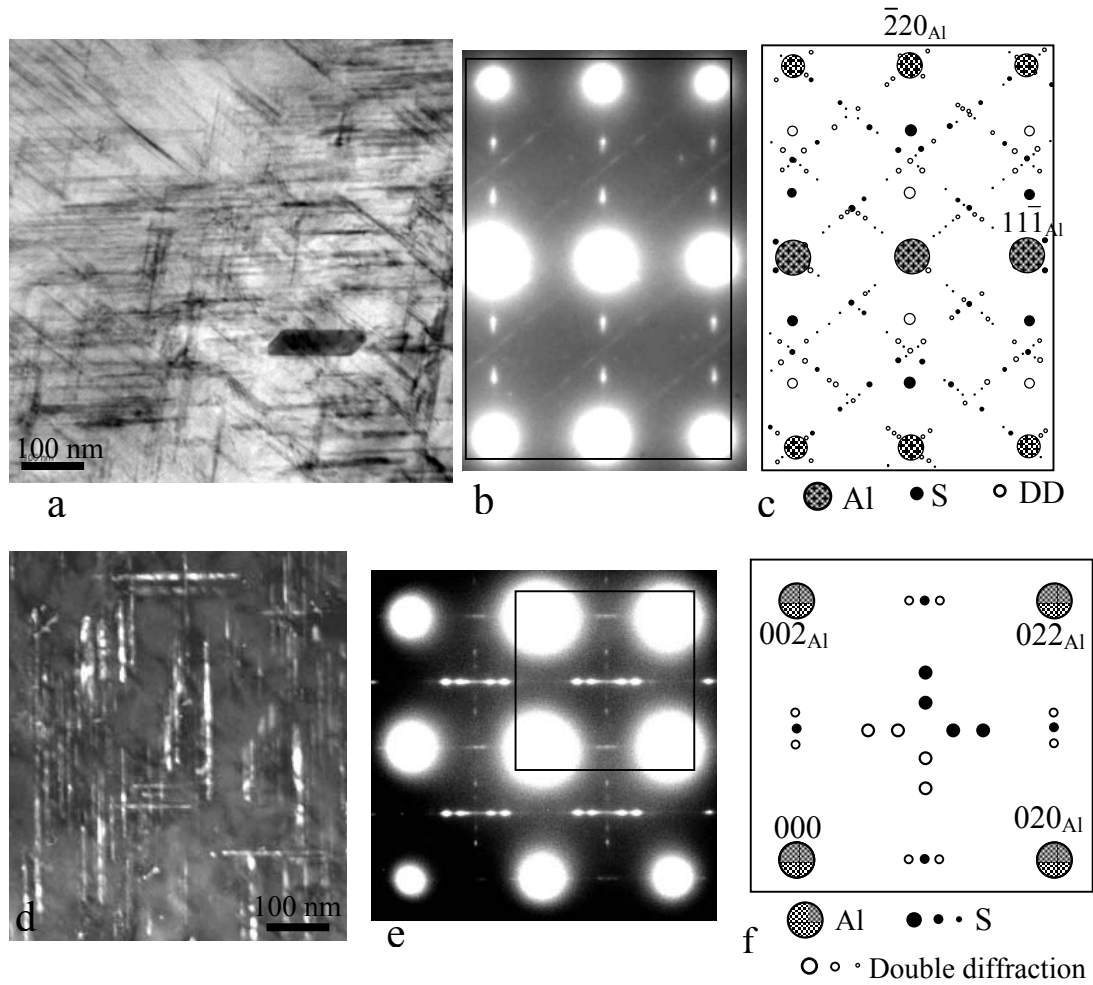


Fig. 2 TEM micrographs and corresponding diffraction patterns of the quenched and stretched Al-2.81Cu-1.05Mg-0.41Mn (wt-%) alloy after ageing at 190°C for (a-c) 6h; (d-f) 12h. (a) bright field; (b) $[112]_{Al}$ SAD pattern; (c) simulated SAD pattern corresponding to Fig. 2b; (d) dark field; (e) $[100]_{Al}$ SAD pattern; (f) simulated SAD pattern corresponding to Fig. 2e.

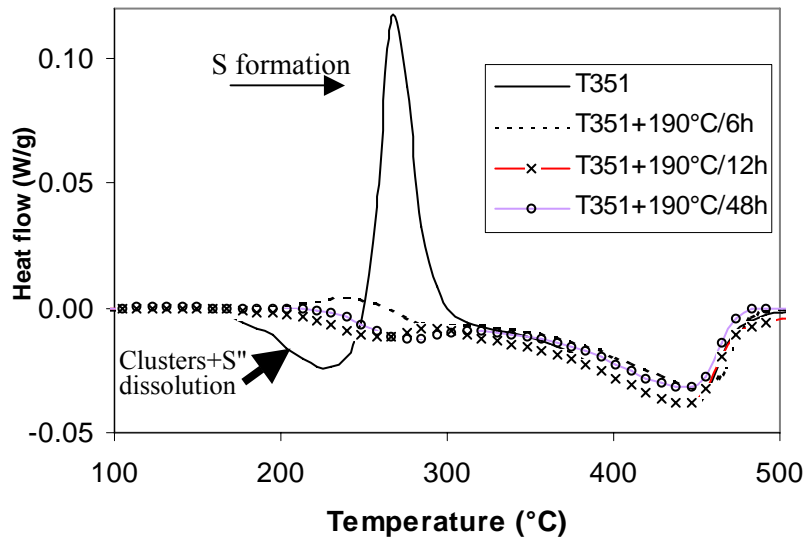


Fig.3 DSC thermogram of Al-2.81Cu-1.05Mg-0.41Mn (wt-%) in quenched and stretched (T351) condition and after subsequent ageing for 6h, 12h and 48 at 190°C.

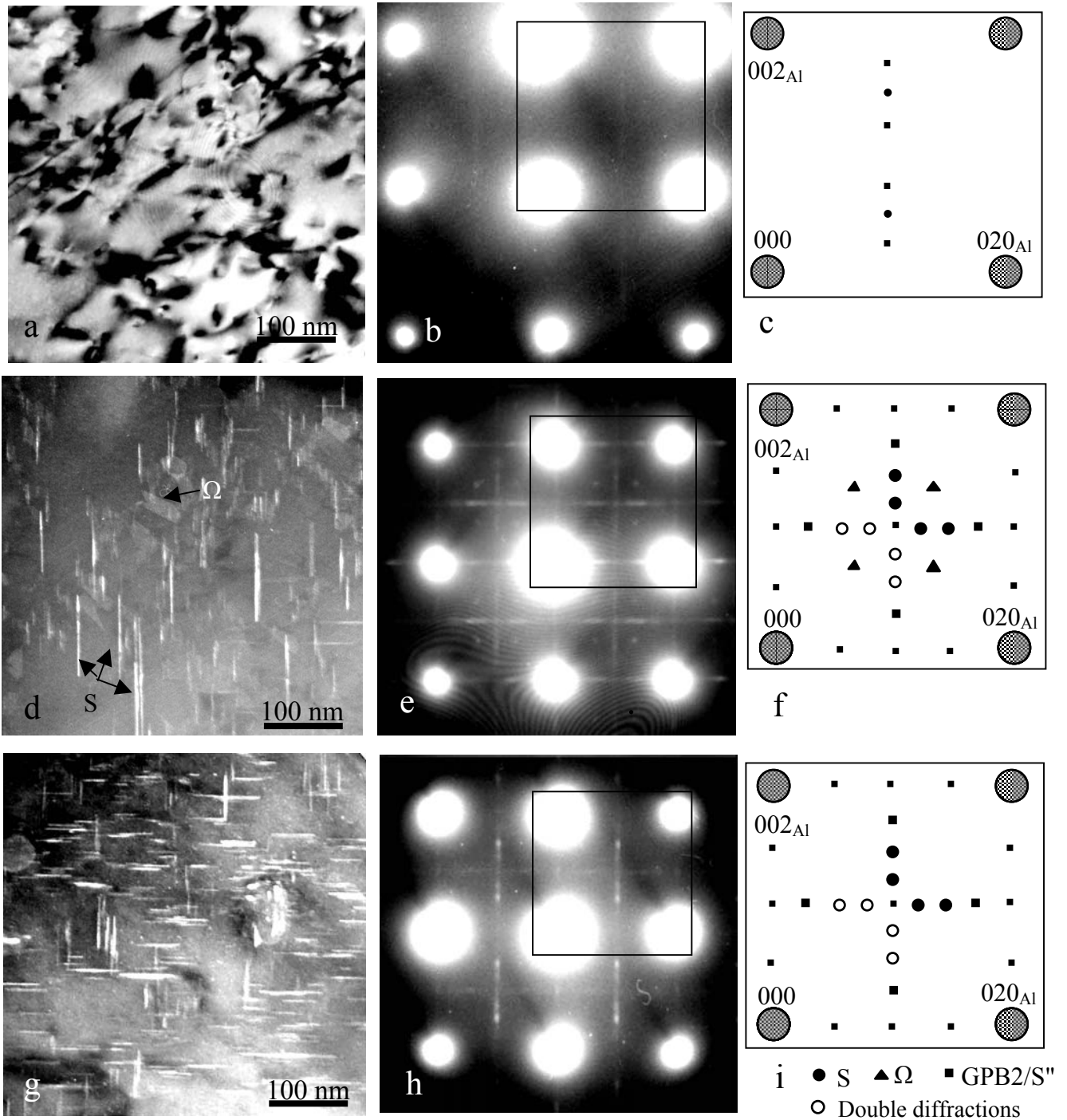


Fig. 4 TEM bright/dark field images, $[100]_{Al}$ diffraction patterns and schematic diagrams (of area indicated in SAD patterns) of the quenched and stretched (T351) Al-2.81Cu-1.05Mg-0.41Mn (wt-%) alloy after ageing at $150^{\circ}C$

(a-c) 24h; (d-f) 48h and (g-i) 72h.

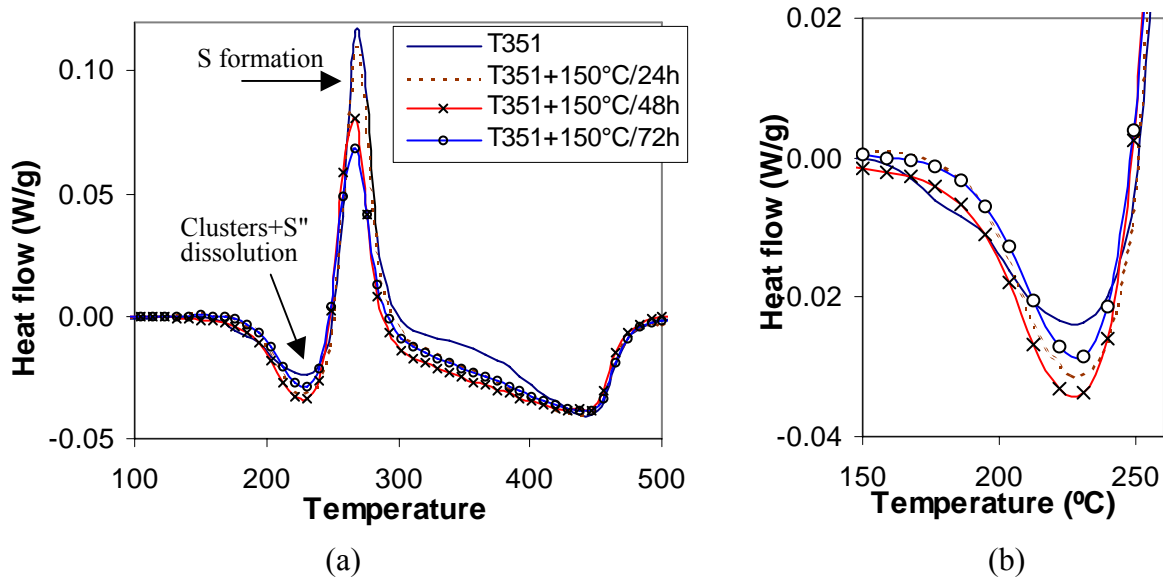


Fig.5 (a) DSC thermogram of Al-2.81Cu-1.05Mg-0.41Mn (wt-%) samples in quenched and stretched (T351) condition and after ageing for 24h, 48h and 72h at 150°C; (b) enlargement of the low temperature dissolution peak in Fig. 5a.